

A COMPACT S – BAND FRONT-END RECTENNA FOR
WIRELESS POWER TRANSFER APPLICATION

IKHWAN PERANGGI POHAN

UNIVERSITI TEKNOLOGI MALAYSIA

A COMPACT S – BAND FRONT-END RECTENNA FOR
WIRELESS POWER TRANSFER APPLICATION

IKHWAN PERANGGI POHAN

A thesis submitted in fulfilment of the
requirements for the award of the degree of
Master of Engineering (Electrical)

Faculty of Electrical Engineering
Universiti Teknologi Malaysia

JANUARI 2006

To my beloved parents

ACKNOWLEDGEMENT

First and foremost, I would like to thank the Creator, ALLAH S. W. T. for giving me such an unbelievable strength to overcome all the obstacles during the completion of this research. In addition, my regards to Prophet Muhammad S.A.W. for guiding men to the straight path.

I would like to express my sincere appreciation to my main supervisor Associate Professor Dr. Mazlina binti Hj Esa for encouragement, guidance, advices and critics. I am also very thankful to my co-supervisor Associate Professor Dr. Jasmy bin Yunus for the valuable support. In addition, many thanks to Mrs. Noor Asniza binti Murad for her support.

I would like to thank all my teachers and lecturers for the shared knowledge. Many thanks to Ms. Rosmawati binti Othman, Mr. Adnall bin Bakar and other technicians for their sincere help. I would like to express thanks to Mr. Mohd. Fairuz bin Mohd. Yusof and all my friends for ideas, help and discussions.

I would also like to thank Dr. Berndie Strassner, Dr. Young-Ho Suh, Dr. Robert Cahill and Dr. Lung-Hwa Hsieh for short warm technical discussions.

Finally, I greatly appreciate my brothers, sisters, Mala and relatives for their spiritual support during my study.

ABSTRACT

A rectenna is used to receive transmitted power through space for wireless power transmission (WPT). This thesis presents the development of an S-band front-end microwave rectenna prototype elements operating at 2.45 GHz of industrial, scientific and medical (ISM) band. The microstrip front-end rectenna consists of an antenna and a low-pass filter (LPF). Both prototype elements were simulated. Optimized designs were fabricated and tested. For the antenna, two designs were investigated, i.e. corner-truncated square patch (CTSP) and slitted CTSP (SCTSP) fed by electromagnetic coupling. Size reduction of 37 % has been achieved through simulations for the SCTSP, compared to CTSP design at the operating frequency of 2.45 GHz. Measurement results showed that the antenna exhibits well matched impedance at the corresponding frequency of operation but with a slight shift of 123 MHz higher frequency as well as 2.5 dB higher axial ratio. SCTSP is proposed for the antenna candidate front-end rectenna. LPF was designed with elliptic function characteristic. Three designs were investigated for single element structure of 3rd order. These were stepped-impedance hairpin (SIH), meandered-gap hairpin (MGH) and over-coupled end meandered-gap hairpin (OCEMGH). Through simulations, size reduction of 28.6 % has been achieved for the MGH, compared to SIH. Both exhibit the same cutoff frequency. It was also found that higher cutoff frequency corresponds to lower insertion loss at 2.45 GHz. An impressive reduction in size of 60 % has been achieved for the OCEMGH, compared to SIH. The OCEMGH also exhibited better insertion loss at 2.45 GHz and rejection at 4.9 GHz and hence is proposed as the filter candidate for the front-end rectenna. Elliptic function LPF of 5th order was also designed. Two designs were proposed, i.e. unidentical cascaded hairpin (UCH) and identical cascaded hairpin (ICH). Simulated results showed that both filter have sharper cutoff frequencies compared to that of SIH. Measurement results showed that the five LPFs agree well with the simulated results.

ABSTRAK

Rektena digunakan untuk menerima kuasa yang dihantar melalui ruang bagi penghantaran kuasa tanpa wayar (WPT). Tesis ini membentangkan pembangunan elemen prototaip rektena gelombang mikro hujung-hadapan jalur-S yang beroperasi pada 2.45 GHz; jalur perindustrian, saintifik dan perubatan (ISM). Rektena mikrojalur hujung-hadapan terdiri daripada antena dan penapis lulus rendah. Kedua-dua elemen prototaip telah disimulasi. Rekabentuk optimum telah dibina dan diuji. Bagi antena, dua rekabentuk diselidiki, iaitu tampalan segi empat sama terpotong-sudut (CTSP) dan tampalan segi empat sama terpotong sudut terkelar (SCTSP). Kedua-duanya mempunyai suapan gandingan elektromagnet. Pengurangan saiz sebanyak 37 % telah diperolehi daripada hasil simulasi untuk SCTSP berbanding CSTP pada frekuensi kendalian 2.45 GHz. Hasil pengukuran menunjukkan bahawa galangan antena terpadan dengan baik pada frekuensi kendalian tetapi terdapat 123 MHz anjakan kecil frekuensi, begitu juga dengan nisbah paksi 2.5 dB yang lebih tinggi. Penapis lulus rendah direkabentuk dengan ciri fungsi eliptik. Tiga rekabentuk dicadangkan untuk element tunggal peringkat ketiga, iaitu pin rambut galangan berlangkah (SIH), pin rambut sela-berliku (MGH) dan pin rambut sela-berliku ganding-hujung-terlebih (OCEMGH). Pengurangan saiz sebanyak 28.6 % telah diperolehi bagi MGH daripada hasil simulasi berbanding SIH. Kedua-duanya mempunyai frekuensi potong yang sama. Frekuensi potong yang lebih tinggi didapati menghasilkan kehilangan sisipan yang lebih rendah pada 2.45 GHz. Pengurangan saiz yang menakjubkan sebanyak 60 % telah diperolehi oleh OCEMGH berbanding SIH. OCEMGH juga menunjukkan kehilangan sisipan pada 2.45 GHz dan penolakan pada 4.9 GHz yang lebih baik dan dicadangkan sebagai calon penapis pada rektena hujung-hadapan. Penapis lulus rendah fungsi eliptik peringkat 5 juga direkabentuk. Dua rekabentuk dicadangkan, iaitu susunan pin rambut kaskad tidak serbasama (UCH) dan pin rambut kaskad serbasama (ICH). Hasil simulasi menunjukkan kedua-dua penapis mempunyai frekuensi potong yang lebih tajam berbanding SIH. Hasil pengukuran menunjukkan bahawa kelima-lima penapis lulus rendah adalah setanding dengan hasil simulasi.

TABLE OF CONTENTS

CHAPTER	TITLE	PAGE
	TITLE	i
	DECLARATION	ii
	DEDICATION	iii
	ACKNOWLEDGEMENT	iv
	ABSTRACT	v
	ABSTRAK	vi
	TABLE OF CONTENTS	vii
	LIST OF TABLES	x
	LIST OF FIGURES	xi
	LIST OF SYMBOLS	xix
	LIST OF ABBREVIATIONS	xxiv
	LIST OF APPENDICES	xxvi
1	INTRODUCTION	1
	1.1 Research Background	1
	1.2 Problem Statement	3
	1.3 Front-end Rectenna Review	3
	1.4 Objective of Research	12
	1.5 Scopes of Research	12
	1.6 Thesis Organization	15
2	BASIC THEORY OF MICROSTRIP ANTENNA AND ELLIPTIC FUNCTION LOW-PASS FILTER	17
	2.1 Introduction	17

2.2	Scattering (S) Parameters and ABCD Matrix	17
2.3	Antenna Properties	20
2.4	Square Patch Microstrip Antenna	25
	2.4.1 Transmission Line Model	26
	2.4.2 Feeding Techniques	28
2.5	Corner-Truncated Square Patch	33
2.6	Compact Microstrip Antenna	32
3	BASIC THEORY OF ELLIPTIC FUNCTION	
	LOW-PASS FILTER	37
3.1	Introduction	37
3.2	Elliptic Function LPF	37
3.3	Coupled Microstrip Lines	41
3.4	Elliptic Function Microstrip LPF	46
4	SLITTED MICROSTRIP ANTENNA DESIGN	51
4.1	Introduction	51
4.2	Square Patch Microstrip Antenna (SP)	51
4.3	Corner-Truncated Square Patch (CTSP_E3)	59
4.4	Slitted Corner-Truncated Square Patch (SCTSP)	65
4.5	SCTSP_E Antenna with Modified Slits	73
4.6	Scaled Prototypes of SCTSP_E3	81
4.7	Summary	85
5	MICROSTRIP HAIRPIN ELLIPTIC FUNCTION LPF	89
5.1	Introduction	89
5.2	Microstrip Stepped Impedance Hairpin (SIH) EF-LPF	90
	5.2.1 Synthesizing lumped elements EF-LPF	90
	5.2.2 Equivalent Circuit Model of SIH	91
	5.2.3 Microstrip SIH EF-LPF Design	96
	5.2.4 Simulation Results, Analysis and Optimization	98
5.3	Meandered-Gap Microstrip Hairpin (MGH) EF-LPF	106
	5.3.1 MGH EF-LPF Design	107
	5.3.2 Simulation Results, Analysis and Optimization	109
5.4	Over-Coupled End EF-LPF	116

5.4.1	Over-Coupled End EF-LPF Design	116
5.4.2	Simulation Results, Analysis and Optimization	118
5.5	Summary	126
6	CASCADED MICROSTRIP HAIRPIN EF-LPF OF HIGHER ORDER	128
6.1	Introduction	128
6.2	Unidentical Cascaded Microstrip (UCH) EF-LPF	128
6.2.1	UCH EF-LPF of 5 th Order Design	130
6.2.2	Simulation Results, Analysis and Optimization	131
6.3	Identical Cascaded Microstrip (ICH) EF-LPF of 5 th Order	138
6.3.1	ICH EF-LPF of 5 th Order Design	139
6.3.2	Simulation Results, Analysis and Optimization	139
6.4	Summary	142
7	MEASUREMENT RESULTS	144
7.1	Introduction	144
7.2	Antenna Measurements	146
7.3	Filters Measurement	151
7.4	Summary	158
7.4.1	SCTSP_E2 Antenna	158
7.4.2	Filters	159
8	CONCLUSION AND RECOMMENDATIONS	161
8.1	Conclusion	161
8.1.1	Antennas	161
8.1.2	Filters	163
8.2	Recommendations	166
	REFERENCES	167
	Appendices A - M	173 - 188

LIST OF TABLES

TABLE NO.	TITLE	PAGE
1.1	Design specification of the antenna	13
1.2	Design specification of the low-pass filter	14
4.1	Optimum dimensions and f_r of SCTSP_E1 and SCTSP_E2	82
4.2	Simulated results of SCTSP_E1, SCTSP_E2 and SCTSP_E3 antennas	85
4.3	Simulated results of the designed antennas	86
5.1	Dimensions of designed MGH with $w_x = 0.65$ mm, $l_x = 0.65$ mm, $l_y = 1.3$ mm and $l_z = 0.25$ mm	111
5.2	Values of f_c and passband insertion loss ripple of the MGH_11, MGH_21, MGH_22 and MGH_32 resonators	112
5.3	f_c and corresponding passband insertion loss ripple for various l_s of the MGH resonator with $l_c = 2.5$ mm	113
5.4	f_c , % f_c decreased and f_c decreased factor of the OCEH_L and OCEH_R	119
5.5	f_c , % f_c decreased and f_c decreased factor of OCEMGH_22_L and OCEMGH_22_R with $l_c = 2.5$ mm, $l_s = 7.3$ mm	121
5.6	Performance of the OCEMGH_21_L with $l_c = 2.05$ mm, $l_s = 6.1$ mm, $l_o = 0.45$ mm and MGH_21 with $l_c = 2.05$ mm and $l_s = 6.6$ mm and SIH of $l_c = 2.65$ mm and $l_s = 7$ mm	126
5.7	Simulated performances of SIH, MGH_22 and OCEMGH_21_L	127
6.1	Simulated passband insertion loss ripple for increasing w_a	136
6.2	Performances of UCHa and ICHa EF-LPF of 5 th order	143
7.1	Performance comparison between measured and simulated results of SCTSP_E2	159
7.2	Performance comparison between measured and simulated results of EF-LPFs	160

LIST OF FIGURES

FIGURE NO.	TITLE	PAGE
1.1	Block diagram of a rectenna circuit connected to a load	2
1.2	(a) Schematic of a half-wave dipole rectenna [3] (b) Dual polarization two orthogonal thin-film dipole antennas of a rectenna [7]	4
1.3	(a) circuit configuration of a 35 GHz dipole rectenna [8] (b) 5.8 GHz dipole rectenna element [9]	5
1.4	(a) Circuit configuration of the dual-frequency dipole rectenna (b) measured frequency responses of the antenna and the antenna with filters [11]	6
1.5	The configuration of dual polarized circular patch rectenna [12]	7
1.6	(a) Cut plane view and configuration of the antenna (b) rectifying circuit configuration [13]	7
1.7	(a) Square patch rectenna with microstrip feed line [14] (b) square patch rectenna with microstrip inset feed line [15]	8
1.8	(a) Configuration of the rectenna with a microstrip circular sector antenna (b) measured return losses of the microstrip circular sector and square patch antennas [16]	8
1.9	The layout of circularly polarized dual-patch antenna [18]	9
1.10	(a) Rectenna block diagram (b) Simulated band-reject filter [19]	10
1.11	The layout of the shorted annular ring-slot rectenna [20]	10
1.12	The structure of corner-truncated square patch rectenna [21]	11
1.13	Geometry of the investigated antennas and filters (not to scale)	14
2.1	Two port network [32]	18
2.2	The ABCD two port network [33]	19
2.3	The dipole antenna with coordinate system [36]	22
2.4	The elliptical polarization [38]	23

2.5	Circular polarization pattern [40]	24
2.6	(a) Rectangular Microstrip patch antenna (b) side view (c) top view [34]	26
2.7	The coaxial feed [47]	29
2.8	Patch with EMC feed [24]	31
2.9	Geometry of a corner-truncated square patch [48]	32
2.10	Geometry of truncated corners square-ring microstrip antenna [49]	34
2.11	Geometry of (a) square microstrip antenna with slits for CP radiation [50] (b) chip resistor loaded rectangular microstrip antenna [51]	35
2.12	Geometry of circularly polarized circular microstrip antenna (a) with tuning stub and (b) with cross slot and tuning stub [52]	36
2.13	Geometry of corner-truncated square patch with four inserted slits [53]	36
3.1	Amplitude-frequency response of a band-pass filter	38
3.2	(a) Comparison of third order Butterworth, Chebyshev and elliptic function filters [54] (b) Normalized elliptic function LPF response [32]	39
3.3	Elliptic function low-pass prototype filters (a) series parallel-resonant branches (b) shunt series-resonant branches [32]	41
3.4	Cross section of a coupled microstrip line [32]	42
3.5	Quasi-TEM modes of a pair of coupled microstrip lines (a) even-mode (b) odd-mode [32]	42
3.6	Stepped-impedance LPF (a) geometry (b) lumped elements EF LPF (c) simulated frequency response [32]	46
3.7	(a) Basic structures of rectangular microstrip element (b) Equivalent circuit (c) Insertion loss response of fifth order [59]	47
3.8	Cross-over and broadside-coupled microstrip line EF-LPF (a) structure (b) equivalent circuit (c) frequency response [61]	48
3.9	Microstrip EF-LPF using slow-wave resonator (a) Geometry (b) lumped elements equivalent circuit (c) frequency response [62]	49
3.10	EF-LPF microstrip SIH resonator (a) geometry (b) equivalent circuit (c) frequency response [63]	50
4.1	The radiating square patch microstrip antenna	52
4.2	Simulated return loss response of SP_C3 (a) $L = 35.23$ mm (b) $L = 35$ mm	53

4.3	Simulated response of SP_C3 with $L = 35$ mm (a) current distribution on the patch (b) observed current distribution along the UU' , VV' and across the XX' , YY'	54
4.4	Simulated radiation patterns of SP_C3 with $L = 35$ mm (a) E - and H -plane (b) RHCP and LHCP	55
4.5	Simulated return loss response of SP_E3 with $L = 35$ mm	56
4.6	Simulated return loss response as decreasing size of the patch	57
4.7	Simulated return loss response for SP3_E with $L = 27.5$ mm	57
4.8	Observed current distribution along UU' , VV' and across XX' , YY' of SP_E3 with $L = 27.5$ mm	58
4.9	Simulated radiation pattern responses of SP_E3 with $L = 27.5$ mm (a) E - and H -plane (b) RHCP and LHCP	58
4.10	Geometry of CTSP_E3 and EMC feed location	59
4.11	Simulated responses of CTSP_E3 with $L = 27.5$ mm and $c = 3.27$ mm (a) return loss (b) RHCP and LHCP patterns at y - z plane (c) AR	60
4.12	(a) AR with decreasing c of CTSP_E3 with $L = 27.5$ mm (b) AR response when $c = 1.875$ mm	61
4.13	Simulated return loss responses of CTSP_E3 with $L = 27.5$ mm and $c = 1.875$ mm	62
4.14	(a) Simulated return loss responses of CTSP_E3 with $L = 27.625$ mm and increasing c (b) Simulated AR of $L = 27.625$ mm and $c = 2$ mm	63
4.15	Simulated response of CTSP_E3 with $L = 27.625$ mm and $c = 2$ mm (a) current distribution (b) observed along UU' , VV' and across XX' , YY'	64
4.16	Simulated radiation patterns in the x - z and y - z plane of CTSP_E3 with $L = 27.625$ mm and $c = 2$ mm	65
4.17	(a) Geometry of SCTSP (b) current distribution on CTSP_E3	66
4.18	Simulated return loss response of SP_E with $L = 23$ mm	66
4.19	Simulated response of SP_E3 with $L = 23$ mm (a) radiation pattern (b) observed current distribution along UU' , VV' and across XX' , YY'	67
4.20	Simulation response of CTSP_E (a) return loss with $c = 1.625$ mm (b) AR with various c	68
4.21	Simulation responses of CTSP_E3 with $L = 23$ mm and $c = 1.625$ mm (a) radiation pattern (b) Observed current distribution along UU' , VV' and across XX' , YY'	69
4.22	Simulated return loss response of SCTSP_E3 with $L = 23$ mm and $c = 1.625$ mm with various l_{sl} sizes. $f_r = 2.932$ GHz, 2.615 GHz, 2.442 GHz and 2.404 GHz for $l_{sl} = 5$ mm, 10 mm,	

	11.2 mm and 11.5 mm, respectively	70
4.23	(a) Relationship of AR with various c of SCTSP_E3 with $L = 23$ mm and $l_{sl} = 11.2$ mm (b) simulated return loss response of SCTSP_E3 with $L = 23$ mm, $l_{sl} = 11.2$ mm and $c = 2.5$ mm	71
4.24	Sense of circular polarization pattern of SCTSP_E3 with $L = 23$ mm, $l_{sl} = 11.2$ mm and $c = 2.5$ mm	72
4.25	Observed current distribution of SCTSP_E3 with $L = 23$ mm, $l_{sl} = 11.2$ mm and $c = 2.5$ mm (a) on the patch (b) along UU', VV' and across XX', YY'	73
4.26	The modified slits (a) clockwise L-shaped slits (CL-SCTSP) (b) counterclockwise L-shaped slits (CCL-SCTSP) (c) direct facing L-shaped slits (DFL-SCTSP) (d) double L-shaped slits (DL-SCTSP)	74
4.27	Simulated responses of CL-SCTSP (a) return loss (b) observed current distribution along UU', VV' and across XX', YY'	75
4.28	Simulated radiation pattern of CL-SCTSP (a) RHCP and LHCP (b) E - and H -planes	76
4.29	Simulated return loss responses of CCL-SCTSP and DFL-SCTSP	77
4.30	Observed current distribution along UU', VV' and across XX', YY' (a) CCL-SCTSP (b) DFL-SCTSP	78
4.31	Simulated CP radiation patterns of (a) CCL-SCTSP (b) DFL-SCTSP	79
4.32	Simulated E - and H -plane radiation patterns of (a) CCL-SCTSP (b) DFL-SCTSP	79
4.33	Simulated return loss response of DL-SCTSP	80
4.34	Observed current distribution along UU', VV' and across XX', YY' of DL-SCTSP	80
4.35	Simulated responses of DL-SCTSP (a) CP radiation patterns (b) AR	81
4.36	Simulated responses of SCTSP_E1 and SCTSP_E2 (a) return loss (b) AR	82
4.37	Observed current distribution of (a) SCTSP_E1 (b) SCTSP_E2	83
4.38	CP radiation patterns of (a) SCTSP_E1 (b) SCTSP_E2	84
5.1	Design Process of the EF-LPF by insertion loss method	90
5.2	Basic geometry of a microstrip SIH resonator [63]	91
5.3	Single transmission line and the equivalent L - C π -type network circuit [32]	91
5.4	Symmetric parallel coupled lines and the equivalent	

	capacitive π -type network circuit [56]	93
5.5	SIH resonator and its L - C equivalent circuit [63]	94
5.6	(a) Compensation of the bend and (b) SIH resonator after chamfering the bends of the single transmission line	95
5.7	Flow chart for designing of microstrip SIH EF-LPF filter	97
5.8	EF-LPF of third order (a) Lumped element values and (b) Simulated return loss and insertion loss responses	98
5.9	Simulated return loss and insertion loss responses of SIH EF-LPF with $l_s = 4.9$ mm and $l_c = 9.4$ mm	99
5.10	Simulated return loss responses of SIH EF-LPF with shortening of l_c when $l_s = 4.9$ mm	99
5.11	Simulated insertion loss responses of SIH EF-LPF with shortening of l_c when $l_s = 4.9$ mm	100
5.12	Relationship of f_c against l_c while maintaining $l_s = 4.9$ mm of SIH LPF	100
5.13	Simulated frequency responses of SIH EF-LPF filter when $l_s = 4.9$ mm and $l_c = 5$ mm (a) return loss and insertion loss (b) passband insertion loss	101
5.14	Simulated frequency responses of SIH EF-LPF filter for various l_s with $l_c = 5$ mm (a) return loss and insertion loss (b) passband insertion loss	102
5.15	Simulated insertion loss responses of SIH EF-LPF filter for various l_s with $l_c = 3.2$ mm (a) passband and stopband (b) passband	103
5.16	Simulated stopband insertion loss responses of SIH EF-LPF filter for various l_s with $l_c = 3.2$ mm	104
5.17	Optimized geometry of microstrip SIH EF-LPF	104
5.18	Optimized microstrip SIH EF-LPF filter (a) simulated return loss and insertion loss responses (b) passband insertion loss response	105
5.19	Typical current distribution of the odd- and even-modes of the coupled microstrip lines [79]	107
5.20	Proposed modified SIH resonator	108
5.21	MGH resonators (a) 1-section (b) 3-section (c) 4-section (d) 5-section	110
5.22	Simulated frequency responses of MGH_ $i1$, MGH_ $i2j1$, MGH_ $i2j2$ and MGH_ $i3j2$ resonators (a) return loss and insertion loss (b) passband insertion loss	111
5.23	Simulated return loss and insertion loss responses of the MGH resonator with $l_c = 2.5$ mm and various l_s	113

5.24	Simulated frequency responses of the MGH EF-LPF of $l_c = 2.5$ mm and $l_s = 7.3$ mm (a) return loss and insertion loss (b) passband insertion loss	114
5.25	Simulated stopband attenuation loss of the MGH EF-LPF $l_c = 2.5$ mm with $l_s = 7.0, 6.8, 6.6$ and 6.4 mm	115
5.26	Simulated frequency response of the MGH EF-LPF of $l_c = 2.5$ mm and $l_s = 6.6$ mm (a) return loss and insertion loss (b) passband insertion loss	115
5.27	Geometries of (a) OCEH LPF with left over-coupled end (OCEH_L) (b) OCEH LPF with right over-coupled end (OCEH_R)	117
5.28	Geometries of (a) OCEMGH_2j2 LPF with left over-coupled end (OCEMGH_L) (b) OCEMGH_2j2 LPF with right over-coupled end (OCEMGH_R)	117
5.29	Geometries of (a) OCEMGH_2j1 LPF with left over-coupled end (OCEMGH_L) (b) OCEMGH_2j1 LPF with right over-coupled end (OCEMGH_R)	118
5.30	Simulated frequency responses of the OCEH_L and OCEH_R (a) return loss and insertion loss (b) passband insertion loss	119
5.31	Simulated frequency responses of the OCEMGH_2j2_L and OCEMGH_2j2_R	120
5.32	(a) Simulated passband insertion loss responses of the OCEMGH_2j2_L and OCEMGH_2j2_R (b) insertion loss of OCEMGH_2j2_L and OCEMGH_2j2_R with $l_o = 1.875$ mm	121
5.33	Simulated return loss and insertion loss responses of the MGH_2j1 with $l_c = 2.05$ mm and $l_s = 6.6$ mm	122
5.34	Simulated frequency responses of the OCEMGH_2j1_L and OCEMGH_2j1_R for $l_c = 2.05$ mm, $l_s = 6.6$ mm and $l_o = 0.45$ mm	123
5.35	Simulated insertion loss responses of OCEMGH_2j1_L with $l_c = 2.05$ mm and l_s shortened (a) passband (b) stopband	124
5.36	Simulated return loss and insertion loss responses of the OCEMGH_2j1_L with $l_c = 2.05$ mm, $l_s = 6.1$ mm and $l_o = 0.45$ mm; MGH_2j1 with $l_c = 2.05$ mm and $l_s = 6.6$ mm, and SIH of $l_c = 2.65$ mm and $l_s = 7$ mm	125
6.1	Asymmetric coupled line (a) geometry (b) equivalent circuit [63]	129
6.2	UCH EF-LPF (a) geometry (b) equivalent circuit	130
6.3	Computed dimensions of the UCH EF-LPF	131
6.4	EF-LPF of 5 th order lumped element values	131
6.5	Simulated frequency responses of the lumped element EF-LPF of 5 th order using <i>Microwave Office</i>	132

6.6	Simulated frequency responses of UCH-EF-LPF filter with $l_{s1} = 6.85$ mm, $l_{c1} = 9.4$ mm, $l_{s2} = 4.4$ mm, $l_{c2} = 9.4$ mm and $w_a = 0.2$ mm	133
6.7	Frequency responses of UCH EF-LPF $l_{s1} = 6.85$ mm, $l_{s2} = 4.4$ mm, $l_{c2} = 9.4$ mm and $w_a = 0.2$ mm with shortening of l_{c1}	133
6.8	Relationship of f_c against the shortening of l_{c1} with $l_{s1} = 6.85$ mm, $l_{s2} = 4.4$ mm, $l_{c2} = 9.4$ mm and $w_a = 0.2$ mm	134
6.9	Frequency responses of UCH EF-LPF $l_{s1} = 6.85$ mm, $l_{c1} = 2.7$ mm, $l_{s2} = 4.4$ mm and $w_a = 0.2$ mm with shortening l_{c2}	134
6.10	Relationship of f_c against the shortening of l_{c2} with $l_{s1} = 6.85$ mm, $l_{c1} = 2.7$ mm, $l_{s2} = 4.4$ mm and $w_a = 0.2$ mm	135
6.11	Simulated frequency responses of UCH EF-LPF with $l_{s1} = 7$ mm, $l_{c1} = 2.7$ mm, $l_{s2} = 5.6$ mm, $l_{c2} = 3.7$ mm and $w_a = 0.2$ mm	135
6.12	Simulated insertion loss responses of UCH EF-LPF with $l_{s1} = 7$ mm, $l_{c1} = 2.7$ mm, $l_{s2} = 5.6$ mm, $l_{c2} = 3.7$ mm and increasing w_a (a) 0 to 10 GHz (b) 7 GHz to 10 GHz	136
6.13	Simulated frequency responses of UCHa and UCHb (a) return loss and insertion loss (b) passband insertion loss	137
6.14	Geometry of ICH EF-LPF of 5 th order	139
6.15	Return loss and insertion loss responses of ICH EF-LPF with $l_s = 7$ mm, $l_c = 2.65$ mm and $w_a = 1.2$ mm	140
6.16	Simulated frequency responses of ICHa and ICHb (a) return loss and insertion loss (b) passband insertion loss	141
6.17	Frequency responses of the optimum UCH and ICH filters	142
7.1	(a) Antenna structure with SMB connector (b) LPF structure with SMA connectors	145
7.2	(a) SCTSP_E2 transmitting antenna (b) Yagi Uda receiving antenna	147
7.3	Measured return loss responses of (a) Yagi Uda array (b) SCTSP_E2	148
7.4	Measured frequency response of the SCTSP_E2	149
7.5	Orientation of the antenna under test	149
7.6	Measured <i>E</i> -plane radiation pattern of SCTSP_E2 with three oriented rotations	150
7.7	Measured <i>H</i> -plane radiation pattern of SCTSP_E2 with three oriented rotations	151
7.8	Measurement set up for insertion loss response of the filters	152
7.9	Measurement set up for return loss response of the filters	153
7.10	Fabricated structures of single EF-LPF (a) SIH (b) MGH_i2j1	

	(c) OCEMGH_ $i2j1$ _L	154
7.11	Fabricated structures of cascaded EF-LPF (a) UCHa (b) ICHa	155
7.12	Measured frequency responses of SIH EF-LPF	155
7.13	Measured frequency responses of MGH_ $i2j2$ EF-LPF	156
7.14	Measured frequency responses of OCEMGH_ $i2j1$ _L LPF	157
7.15	Measured frequency responses of UCHa EF-LPF	157
7.16	Measured frequency responses of ICHa EF-LPF	158

LIST OF SYMBOLS

A	:	Voltage ratio
a_1	:	Incident wave at port 1
a_2	:	Incident wave at port 2
ABCD	:	Matrix parameters
a_n	:	Incident wave at port n
B	:	Transfer impedance
b_1	:	Reflected wave at port 1
b_2	:	Reflected wave at port 2
b_n	:	Reflected wave at port n
c	:	Length of the perturbation section
c'	:	Speed of light
C	:	Transfer admittance
C_{3s}	:	Total capacitance of adjacent transmission line and shunt capacitances of hairpin resonator 1 and 2
C_a	:	Equivalent capacitance of the adjacent single transmission line
C_e	:	Even-mode capacitance
C_f	:	Fringe capacitance at the outer edge of the strip
C_f'	:	Fringe capacitance due to the presence of another line
C_g	:	Equivalent gap capacitance of coupled line
C_{ga}	:	Fringe capacitance for the air across the coupling gap
C_{gd}	:	Fringe capacitance for dielectric regions across the coupling gap
C_n	:	Scaled capacitor element
C_o	:	odd-mode capacitance
C_p	:	Parallel plate capacitance between the strip and ground plane
C_p	:	Equivalent shunt capacitance of coupled line
C_{p1}	:	Equivalent shunt capacitance of coupled line of resonator 1
C_{p2}	:	Equivalent shunt capacitance of coupled line of resonator 2

C_{ps}	:	Sum of the capacitance of single transmission line, coupled line and step width discontinuity
C_s	:	Equivalent capacitance of single transmission line
C_{s1}	:	Equivalent capacitance of single transmission line of resonator 1
C_{s2}	:	Equivalent capacitance of single transmission line of resonator 2
C_{Δ}	:	Step width discontinuity
d	:	Maximum dimension of antenna
D	:	Current ratio
E	:	Electric field
E_x	:	Electric field in x direction
E_y	:	Electric field in y direction
f_c	:	Cutoff frequency
f_{c2}	:	$ S_{21} $ 3-dB point again after f_c
f_{cCP}	:	Frequency with minimum axial ratio
f_H	:	Higher cutoff frequency
f_L	:	Lower cutoff frequency
f_r	:	Operating frequency
G_r	:	Radiation conductance
g_0	:	Input terminal impedance
g_{Cn}	:	Prototype element value of capacitor
g_{Ln}	:	Prototype element value of inductor
g_{n+1}	:	Output terminal impedance
H	:	Magnetic field
h	:	Thickness of substrate
i	:	Numbers of the corrugated in the left line of the coupled line
I_1	:	Current at port 1
I_2	:	Current at port 2
I_L	:	Insertion loss between ports n and m
j	:	Numbers of the corrugated in the right line of the coupled line
L	:	Length of patch
L_A	:	Insertion loss
L_t	:	perturbed side length
L_1	:	Distance from feed point to the left edge of the patch
L_2	:	Distance from feed point to the right edge of the patch
l_a	:	length between bottom-left-end-gap and the nearest meander section
l_b	:	length between top-left-end-gap and the nearest meander section

l_d	:	length between bottom-right-end-gap and the nearest meander section
l_e	:	length between top-right-end-gap and the nearest meander section
l_x	:	length of external meander section
l_y	:	axial length of longer meander section
l_z	:	length of internal meander section
L_{Ar}	:	Passband ripple
L_{As}	:	Minimum stopband insertion loss
l_c	:	Length of the coupled line
l_{c1}	:	Length of the coupled line of resonator 1
l_{c2}	:	Length of the coupled line of resonator 2
L_n	:	Scaled inductor element
l_o	:	Length of the over-coupled end
L_s	:	Equivalent inductance of single transmission line
l_s	:	Length of single transmission line
l_{s1}	:	Length of single transmission line of resonator 1
l_{s2}	:	Length of single transmission line of resonator 2
l_{sl}	:	Length of slit
n	:	Filter order
OA	:	Major axis
OB	:	Minor axis
P_{dB}	:	Cross polar level
P_{roc}	:	Open circuit reflected power
P_{rsc}	:	Short circuit reflected power
P_r	:	Device under test reflected power
P_i	:	Input power
P_1	:	Power from direct connection
P_2	:	Output power from inserted device
Q	:	Quality factor
R	:	Far-field distance
R_L	:	Return loss at port n
S'	:	Total area of the patch
S	:	Band designation for 2 GHz to 4 GHz
s	:	Gap of the coupled line
s'	:	Overlap distance of EMC feed
S	:	Scattering
S_{11}	:	Input reflection coefficient

S_{12}	:	Reverse transmission coefficient
S_{21}	:	Forward transmission coefficient
S_{22}	:	Output reflection coefficient
t	:	Thickness of conductor
V_1	:	Voltage at port 1
V_2	:	Voltage at port 2
W	:	Width of patch
w	:	Width of microstrip line
w_a	:	Width of the adjacent single transmission line
w_c	:	Width of coupled lines
w_s	:	Width of single transmission line
w_{sl}	:	Width of slit
w_x	:	axial width of shorter meander section
Y_c	:	Admittance of equivalent capacitance of single
Y_g	:	Admittance of gap capacitance of coupled lines
Y_L	:	Admittance of equivalent inductance of single
Y_p	:	Admittance of shunt capacitance of coupled lines
Y_s	:	Admittance of single transmission line
Z_0	:	Characteristic impedance
Z_{0e}	:	Even-mode characteristic impedance
Z_{0o}	:	Odd-mode characteristic impedance
Z_{in}	:	Input impedance
Z_L	:	Impedance of inductor
Z_s	:	Characteristics impedance of the single transmission line
ΔL	:	Line extension
Δs	:	Total area of the perturbation segment
β_c	:	Phase constant of the coupled line
β_e	:	Phase constant of even-mode
β_g	:	Propagation constant
β_o	:	Phase constant of odd-mode
β_s	:	Phase constant of the single transmission line
ε	:	Ripple constant
ε_r	:	Relative dielectric constant
ε_{re}	:	Effective dielectric constant
ε_{re}^e	:	Effective dielectric constant of even-mode

ε_{re}^o	:	Effective dielectric constant of odd-mode
ε_{rt}	:	Total dielectric constant
Γ	:	Reflection coefficient
λ	:	Wavelength
λ_0	:	Free space wavelength
τ	:	Tilt angle of the ellipse
δ	:	Loss tangent
Ω	:	Frequency (rad/s)
Ω	:	Ohms
Ω_c	:	Cutoff frequency
Ω_{c1}	:	Low cutoff frequency
Ω_{c2}	:	High cutoff frequency
Ω_s	:	Ratio of equal-ripple stopband starting to cutoff frequency
ω	:	Angular frequency
ω_c	:	3-dB cutoff angular frequency
θ	:	Elevation angle
φ	:	Azimuth angle

LIST OF ABBREVIATIONS

AR	:	Axial ratio
BPF	:	Band-pass filter
BW	:	Bandwidth
CCL-SCTSP	:	Counterclockwise L-shaped slits SCTSP
CIR	:	Circulator
CL-SCTSP	:	Clockwise L-shaped slits SCTSP
CP	:	Circular polarization
CPS	:	Coplanar strip line
CTSP	:	Corner-truncated square patch
dB	:	Decibel
dBd	:	Decibel over half-wave dipole radiator
dB _i	:	Decibel over isotropic radiator
DFL-SCTSP	:	Direct facing L-shaped slits SCTSP
DL-SCTSP	:	Double L-shaped slits SCTSP
DRLA	:	Dual rhombic loop antenna
DVM	:	Digital voltmeter
EDA	:	Electronic design automation
EF	:	Elliptic function
EM	:	Electromagnetic
EMC	:	Electromagnetic coupling
HPBW	:	Half power beamwidth
ICH	:	Identical cascaded hairpin
ISM	:	Industrial, scientific and medical
LHCP	:	Left-hand circularly polarized
LPF	:	Low-pass filter
MGH	:	Meandered-gap hairpin
OCEH	:	Over-coupled end hairpin

OCEH_L	:	Left over-coupled end hairpin
OCEH_R	:	Right over-coupled end hairpin
OCEMGH_L	:	Left over-coupled end meandered-gap hairpin
OCEMGH_R	:	Right over-coupled end meandered-gap hairpin
OP-AMP	:	Operational Amplifier
PCB	:	Printed circuit board
Rectenna	:	Rectifying antenna
RHCP	:	Right-hand circularly polarized
SCTSP	:	Slitted corner-truncated square patch
SCTSP_C	:	SCTSP fed by coaxial feed
SCTSP_E	:	SCTSP fed by electromagnetic coupling feed
SIH	:	Stepped-impedance hairpin
SP	:	Square Patch
TEM	:	transverse electromagnetic
UCH	:	Unidentical cascaded hairpin
VCO	:	Voltage controlled oscillator
VSWR	:	Voltage standing wave ratio
WPT	:	Wireless power transmission

LIST OF APPENDICES

APPENDIX	TITLE	PAGE
A	ABCD parameters of some useful two-port circuits [33]	173
B	Element values for Elliptic function low-pass prototype filters ($g_0 = g_{n+1} = 1$, $\Omega_c = 1$, $L_{Ar} = 0.1$ dB) [32]	174
C	Data sheet of board material [64]	175
D	Square patch microstrip antenna dimensions	176
E	Calculation of 50 Ohms impedance transmission line for EMC feed	177
F	Calculation of impedance and frequency scaling of 3 rd order EF-LPF	178
G	Calculation of the characteristic impedance of the single transmission line and the even- and odd-mode impedance of the coupled lines of the stepped impedance hairpin EF-LPF	179
H	Calculations of MGH	182
I	Calculation of impedance and frequency scaling of 5 th order EF-LPF	184
J	Normalized radiation patterns of <i>E</i> - and <i>H</i> -planes for three rotated orientation of SCTSP_E2	185
K	Voltage – Power calibration curves of MST532 set-up [30]	186
L	VCO characteristic calibration graph of MST532 set-up [30]	187
M	List of publication	188

CHAPTER 1

INTRODUCTION

1.1 Research Background

A wireless power transmission (WPT) system refers to a system whereby electric power is transmitted from one point to another through the vacuum of space or the earth's atmosphere without the use of wires or any substance. The power in space would be in microwave or laser beams. The laser has an advantage of having small beam divergence. However, the efficiencies in generating the laser beam and converting it back into electrical energy are low compared with microwave [1, 2]. Therefore, the development of power transmission system using microwave beam is more attractive.

WPT is one of the most useful applications of radio waves. The concept of beamed microwave power transmission is important where it is not feasible to transmit power from one place to another by traditional transmission and distribution system. The most abundant and sustainable source of energy for mankind is the sun. Solar energy is difficult to be used directly on earth, because of its low density, and its lack of regularity due to weather condition and day-and-night cycles. To solve this problem, Glaser proposed an idea of orbiting satellites in geosynchronous

equatorial orbit to collect the unlimited sunlight, converting the solar energy and transmitting the energy through microwave to earth, called Solar Power Satellites (SPS) [2]. On the earth, the microwave will be rectified and transformed to utility power for public use. This power then can be transmitted wireless from one point to another directly or by power relay satellites through microwave.

Malaysia has a large area of relatively undeveloped land near the equator in Sarawak where many people still live without electricity. Because of this, Malaysia is a potential place to be a rectenna site. The WPT is also an alternative method of energy transmission in Malaysia. In addition, the UTM Skudai campus has been identified as a rectenna test bed for implementing the WPT concept. The campus is located very near to the equator.

One of the key components in a WPT system is a rectenna at the receiving end [3, 4]. The block diagram of a rectenna is shown in Figure 1.1 which consists of an antenna, low-pass filter (LPF) and rectifying circuits. The front-end of a rectenna is an antenna and LPF. The LPF inserted between the antenna and the rectifying circuit needs to be designed so that the fundamental frequency can be passed and a portion of the higher order harmonics generated from the rectifying circuit be rejected back to the rectifying circuit [5].

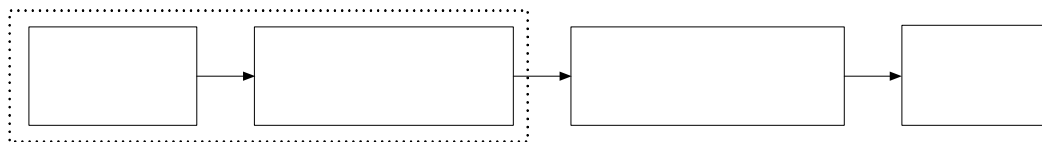


Figure 1.1 Block diagram of a rectenna circuit connected to a load.

1.2 Problem Statement

Power can be wirelessly delivered from one point to another by using microwave frequency. In a WPT system, a rectenna is used to receive the transmitted power through space and converting the power to dc power, hence, it can be used for energy storage. Two important components of the front-end rectenna are the receiving antenna and the adjacent low-pass filter. There is an immediate need to develop a single front-end rectenna prototype which is useful for terrestrial WPT reception.

To eliminate the need to orient the antennas between the transmitter and the receiver, the receiving antenna has to be circularly polarized. Hence, the rectenna may be rotated without significantly changing the output voltage. Besides that a compact antenna is desired which corresponds to lightweight device and cost effectiveness of fabrications.

Low passband insertion loss, sharp cutoff frequency steepness and high stopband rejections are desirable elliptic function filter response. Beside that, compactness in the design is desirable for cost effectiveness of fabrications.

1.3 Front-end Rectenna Review

Since the early 1960s, rectennas have been researched and developed. Brown was a pioneer in developing the first 2.45 GHz rectenna [3]. The front-end rectenna consists of an aluminium bar half-wave dipole antenna and LPF. Besides being a filter, the LPF is used as an impedance matching between the antenna and the rectifying circuit. Figure 1.2(a) shows the schematic of the rectenna. Later, Brown

and Triner [6] developed a thin-film printed –circuit dipole rectenna to reduce the weight. In [7], dual polarization rectenna was developed to receive power from transmitted beam of two orthogonal polarizations. Hence, the power received will be maximum. The antenna was realized by two thin-film dipole orthogonal linearly polarized foreplane in X and Y orientations separated by a multiple of half-wavelength distance to achieve dual polarization as shown in Figure 1.2(b). The basic antenna was employed from [6]. However, this geometry has a bulky structure due to using two orthogonal antennas to achieve dual polarization.

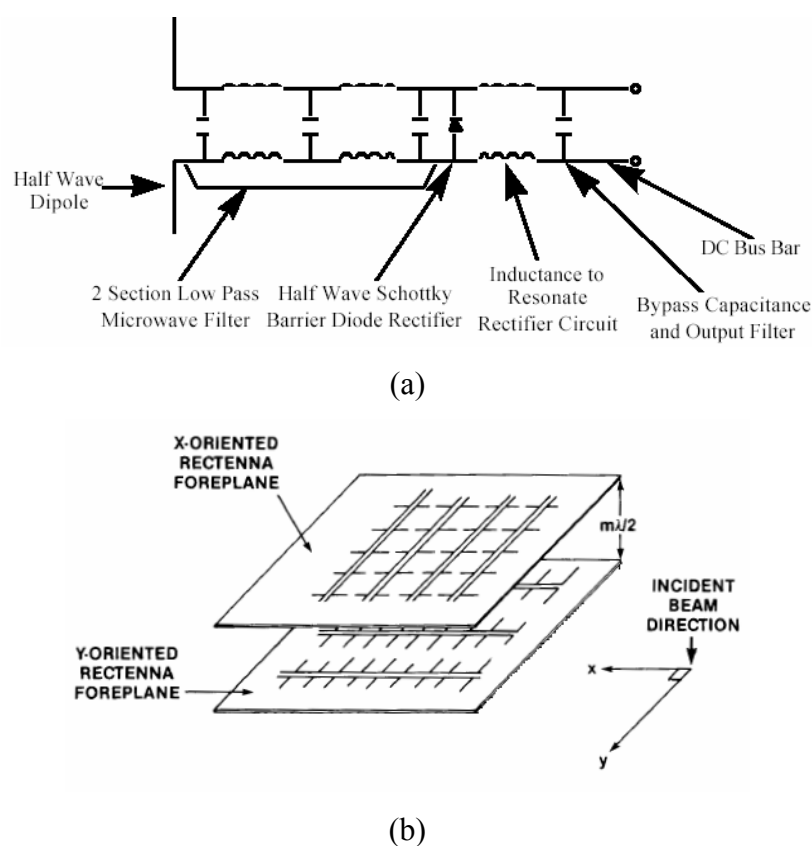


Figure 1.2 (a) Schematic of a half-wave dipole rectenna [3] (b) Dual polarization two orthogonal thin-film dipole antennas of a rectenna [7].

A rectenna element using a microstrip dipole antenna operating at 35 GHz has been developed [8]. Figure 1.3(a) shows the circuit configuration of the rectenna. The rectenna has a coplanar strip line LPF which consists of three transmission line sections to connect the antenna and the rectifying circuit. The LPF is of a stepped-impedance LPF having a Butterworth or Chebyshev response. The

rectenna in this design has two filter sections similar to [3, 6, 7]. The LPF structure is space consuming.

A dipole rectenna has been developed by [9, 10]. In [9], the rectenna operates at 5.8 GHz and is shown in Figure 1.3(b). In this design, the LPF composed of three printed strips on the opposite of the coplanar strip line transmission line. The rectenna has only one section of LPF and the coplanar strip line has an advantage of allowing ease mounting of the rectifying circuit devices. The cutoff frequency of the LPF was located between the fundamental frequency (to pass the operating frequency) and the second order harmonic (to reject the higher harmonics). The design of a single section LPF is interesting as the whole design can be made compact. The filter proposed in this thesis employs such design.

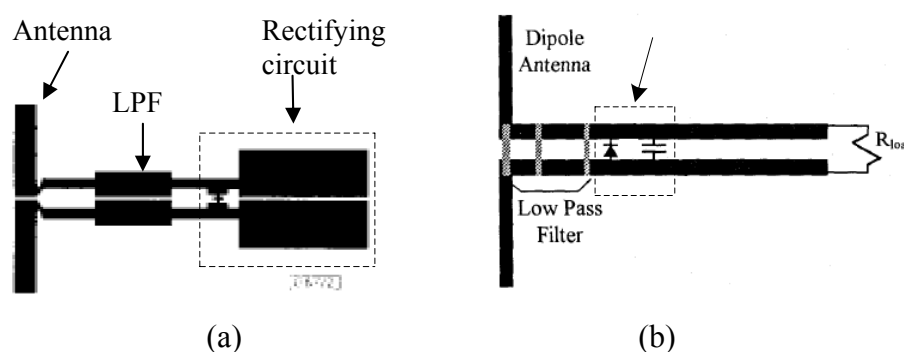


Figure 1.3 (a) circuit configuration of a 35 GHz dipole rectenna [8] (b) 5.8 GHz dipole rectenna element [9].

A dual-frequency printed dipole rectenna has been developed for WPT at 2.45 GHz and 5.8 GHz [11]. The antenna consists of 2 dipoles as shown in Figure 1.4(a). The long dipole operates at 2.45 GHz while the short dipole operates at 5.8 GHz. The filter circuit in this design has a coplanar strip line (CPS) LPF integrated with a bandstop filter. The LPF has a cutoff frequency of 7 GHz to pass 2.45 GHz and 5.8 GHz frequencies while rejects 11.6 GHz which is the second order harmonic of 5.8 GHz. However, the LPF will also pass the 4.9 GHz and 7.35 GHz frequencies which are the second and third order harmonics of 2.45 GHz. To reject these harmonics, a bandstop filter is introduced to the filter circuit. The measured

frequency responses of the antenna and the antenna with filter are shown in Figure 1.4(b). This rectenna can be used for WPT at either frequency depending upon power availability at 2.45 GHz or 5.8 GHz. However, the presence of two filters increases the bulkiness of the rectenna.

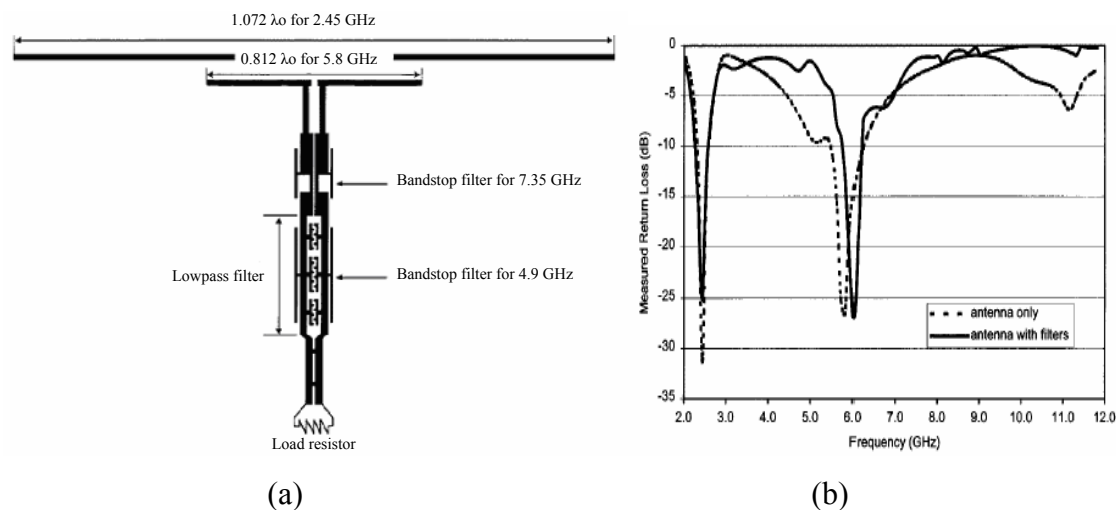


Figure 1.4 (a) Circuit configuration of the dual-frequency dipole rectenna
(b) measured frequency responses of the antenna and the antenna with filters [11].

A circular patch antenna has been designed for dual polarized rectenna at 2.45 GHz [12]. The antenna is fed 90° apart by two transmission line feeds at the edges of the antenna to achieve dual polarization as shown in Figure 1.5. The LPFs are attached at the two feed lines. The LPFs can be the stepped-impedance LPF having a Butterworth or Chebyshev response. This configuration, however, increases the bulkiness of the front-end rectenna.

A circular patch was also employed [13]. Figure 1.6 shows the configuration and the cut plane view of the rectenna. The rectenna was constructed on two layer substrates and operates at 5.8 GHz. The antenna was fed by a pin near the centre of the patch to minimize the area of the feeding circuit and leads to a linearly polarized. In this design, the LPF was included in the rectifying circuit and placed at the rear side of the rectenna. The LPF is of stepped-impedance as shown in Figure 1.6(b).

The overall thickness of the rectenna element is 2.4 mm which is slightly bulky for mobile application. In addition, the feed pin increases the difficulty of fabrication and decrease the cost effectiveness of the rectenna.

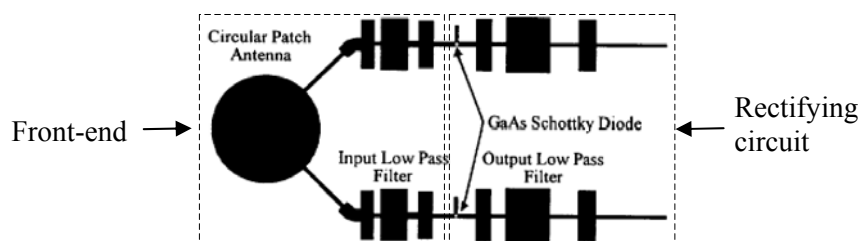


Figure 1.5 The configuration of dual polarized circular patch rectenna [12].

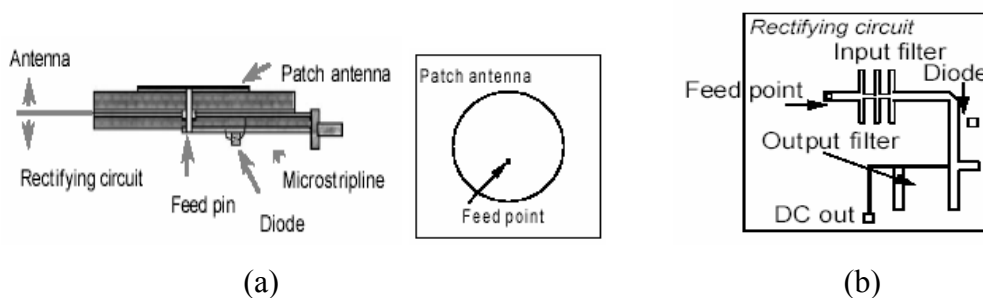


Figure 1.6 (a) Cut plane view and configuration of the antenna (b) rectifying circuit configuration [13].

A square patch microstrip antenna has been employed to construct the rectenna [14]. The antenna was fed by a microstrip line. Microstrip LPF of 3rd order with Chebyshev response was used as the filter. The disadvantage of this design is its microstrip antenna patch size. Figure 1.7(a) shows the configuration of the rectenna element. A similar square patch was developed with an inset feed microstrip line to reduce the size of the rectenna [15]. It was found that the inset does not significantly affect the resonant frequency but it modified the input impedance. However, this design does not have a filter circuit to block the higher harmonics from the rectifier circuit which leads to degradation of the rectenna performance. Figure 1.7(b) shows the corresponding rectenna layout.

A rectenna designed with a microstrip harmonic-rejecting circular sector antenna at 2.4 GHz has been proposed [16, 17]. Compared to the square patch antenna, the circular sector antenna using inset feed exhibits high reflection coefficient at the second and third harmonics. Because of this, the LPF between the antenna and rectifying circuit can be eliminated. In addition, the antenna exhibits linearly polarized wave. The configuration of the rectenna with a microstrip circular sector antenna and the measured return losses of the microstrip circular sector and square patch antennas are shown in Figure 1.8.

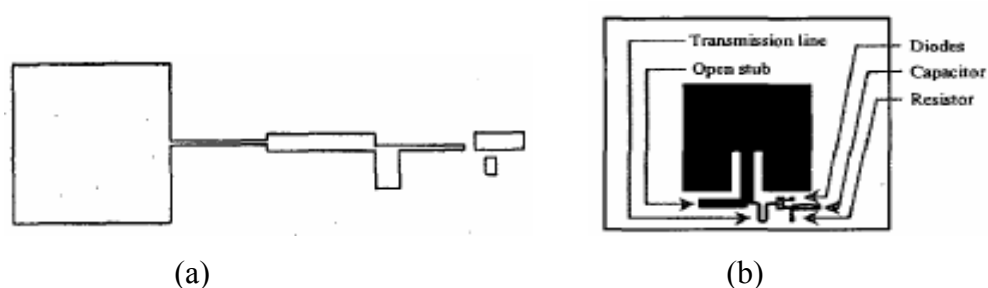


Figure 1.7 (a) Square patch rectenna with microstrip feed line [14]
(b) square patch rectenna with microstrip inset feed line [15].

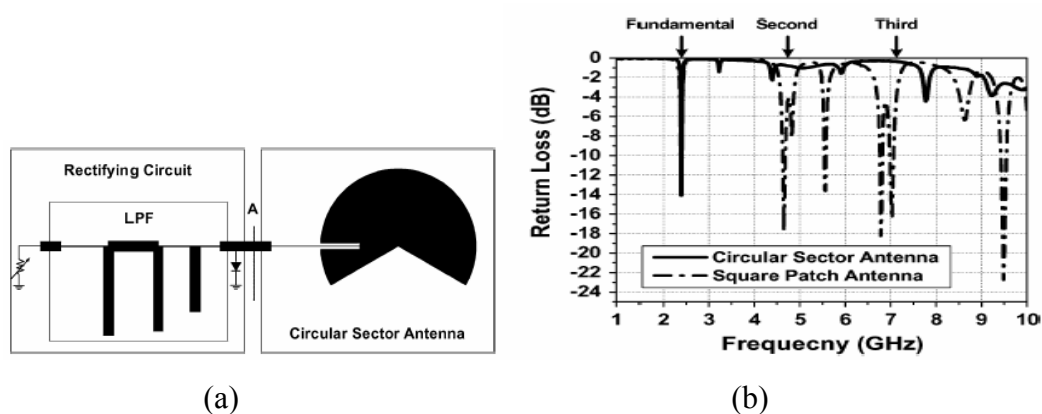


Figure 1.8 (a) Configuration of the rectenna with a microstrip circular sector antenna (b) measured return losses of the microstrip circular sector and square patch antennas [16].

In the last seven years, researchers have been focused on circularly polarized rectenna. Compared to the linearly or dual polarization, the circular polarization can eliminate the need to orient the antenna, reduce the effects of multipath and maximize the received signal. Hence, the rectenna can be rotated while maintaining receiving constant power. Planar dual-patch antenna has been used to achieve circularly polarized rectenna [18]. Dual identical almost quadratic patch has been proposed. Figure 1.9 shows the layout of the circularly polarized dual-patch rectenna. However, the rectenna is bulky due to having two patch antennas and has no LPF to reject the higher harmonics flowing back into the antenna.

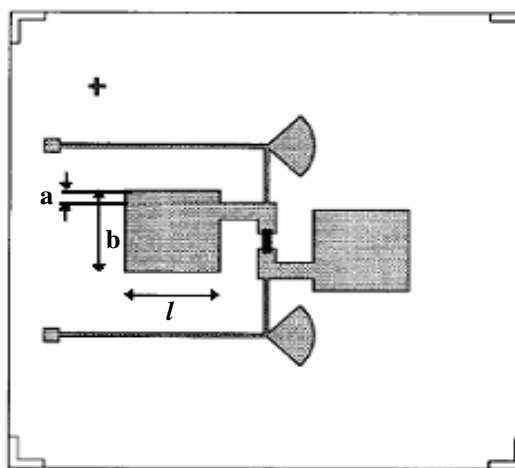


Figure 1.9 The layout of circularly polarized dual-patch antenna [18].

A 5.8 GHz rectenna using a dual rhombic loop antenna (DRLA) has been developed [19]. This antenna exhibits circular polarization. Circular polarization is achieved by having two gap positions of DRLA. The positioning of the gaps, as shown in Figure 1.10, yields left-hand circular polarization. If the gaps are mirrored to the opposing sides of the antenna, the DRLA will become a right hand circular polarization. The CPS tuning stubs tune out the imaginary impedance in order to yield a real impedance at the antenna's input terminals and allow single rectenna element to be connected to other rectennas to form an array. The advantages for using DRLA are high gain, wideband performance and fabrication simplicity. The rectenna used a CPS band-reject filter to suppress the reradiated harmonics flowing from the diode to the antenna. Figure 1.10 shows the rectenna block diagram and the

simulated band-reject filter frequency response. The focused harmonic to be suppressed by the filter is the second harmonic. This is because higher harmonics are not significant as the second harmonic [5]. However, the CPS band-reject filter has a complicated design structure.

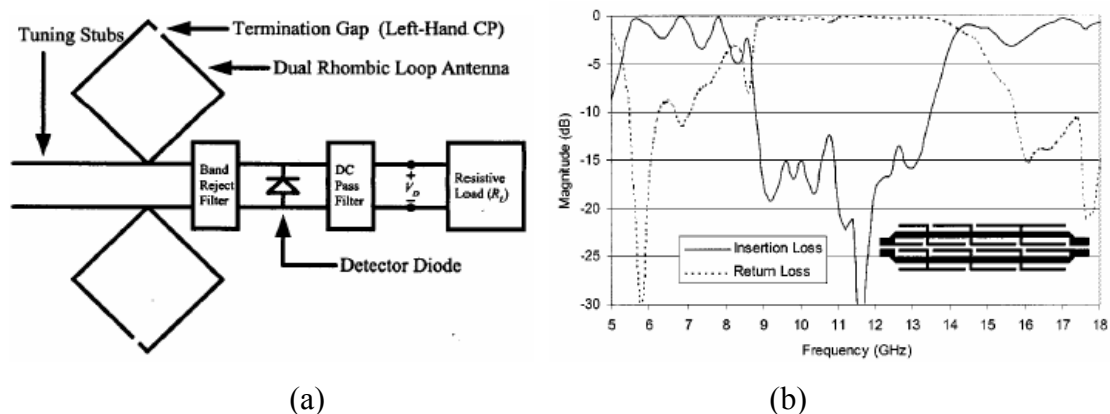


Figure 1.10 (a) Rectenna block diagram (b) Simulated band-reject filter [19].

A circularly polarized rectenna using a shorted annular ring-slot antenna operating at 5.8 GHz has been proposed [20]. Figure 1.11 shows the layout of the rectenna. The antenna is fed from the bottom layer with a transmission line and two quarter-wave transformers to match to the rectifier circuit. This leads to increasing the size of the rectenna. In addition, the rectenna does not have any filter circuit between the antenna and the rectifier circuit for filtering out the higher order harmonics.

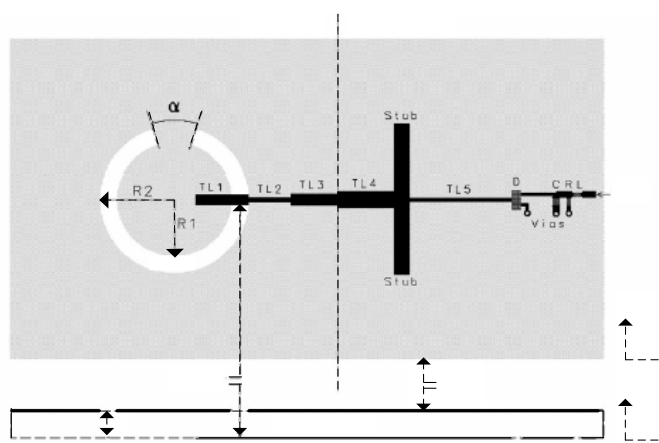


Figure 1.11 The layout of the shorted annular ring-slot rectenna [20].

A circularly polarized rectenna using a corner-truncated square patch has been developed [21, 22]. Figure 1.12 shows the rectenna structure in [21]. The LPF between the antenna and the rectifying circuit has a Chebyshev response. This is a stepped-impedance LPF of 5th order. The advantage of corner-truncated square patch is that the circular polarization can be achieved by a single feed which leads to reducing the size of the rectenna. Such patch is attractive and the design is further modified and proposed in this thesis.

Various operating frequencies of rectennas have been used by various researchers. The conventional operating frequency is 2.45 GHz, located in the industrial, scientific and medical (ISM) band. Later, the higher ISM band 5.8 GHz is proposed as the operating frequency to decrease the size of the antenna. However, increasing the operating frequency further beyond 10 GHz will also increase severe problems of attenuation in rain and clouds and diminishing efficiency [23]. The operating frequency of 35 GHz has smaller aperture areas, however, the components necessary for generating high power at 35 GHz are inefficient and expensive [8]. The 2.45 GHz has advantages of excellent compromise in transmission through the Earth's atmosphere. Furthermore, the components and the technology are the most advanced at 2.45 GHz.

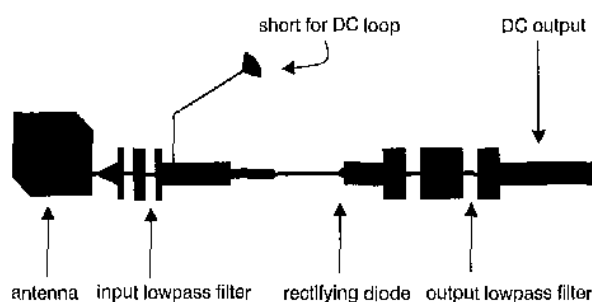


Figure 1.12 The structure of corner-truncated square patch rectenna [21].

The antenna proposed in this thesis focuses on having circular polarization due to the advantages as previously mentioned. The design in [21] is employed and extended. Some modifications were made and investigated for better performance.

The antenna structure was perturbed to obtain a compact configuration. Two antenna feeds were considered; coaxial probe and electromagnetic coupling (EMC) feeds. The EMC feed has an advantage of reducing the spurious radiation from various transmission line discontinuities and eliminating the physical connection between the antenna and the feed line [24]. Furthermore, since most of the LPF between antenna and the rectifying circuit used Chebyshev stepped-impedance microstrip LPF, the elliptic function LPF in microstrip structure is proposed in this thesis to reduce the size of the structure but with high rejection in the attenuation band. The LPF focuses on suppressing the second harmonic of the operating frequency, similar to [5, 19, 25].

1.4 Objective of Research

The objective of the research is to design and develop a single S-band front-end rectenna (rectifying antenna) prototype elements operating at 2.45 GHz which consists of an antenna and an LPF for blocking the higher harmonic frequencies.

1.5 Scopes of Research

The scopes of the research are as follows:

- (i) Design of linearly polarized square patch antenna with two types of feed; coaxial feed and electromagnetic coupling (EMC) feed.
- (ii) Design of circularly polarized corner truncated square patch antenna with EMC feed.
- (iii) Design of modified circularly polarized corner-truncated square patch antenna with EMC feed.

- (iv) Design of single element stepped impedance hairpin elliptic function (EF) LPF.
- (v) Design of single element modified stepped-impedance hairpin EF-LPFs having meandered-gap and over-coupled end.
- (vi) Design of cascaded hairpin EF-LPF based on the single element designs.
- (vii) Simulate all the designed antennas and filters.
- (viii) Measure the optimum designed antenna and filters.

Calculations were carried out using *Mathcad* 2000 [26] while *Microwave Office* 2003 v.6.0 Demo Version [27] was used for simulating the lumped elements of the LPF. *Sonnet Suites* v.9 [28] was used for simulating the microstrip structures of the antennas and LPFs. Measurements were performed using AntennaLab [29] and MST532 [30], for the optimum antenna and LPFs, respectively.

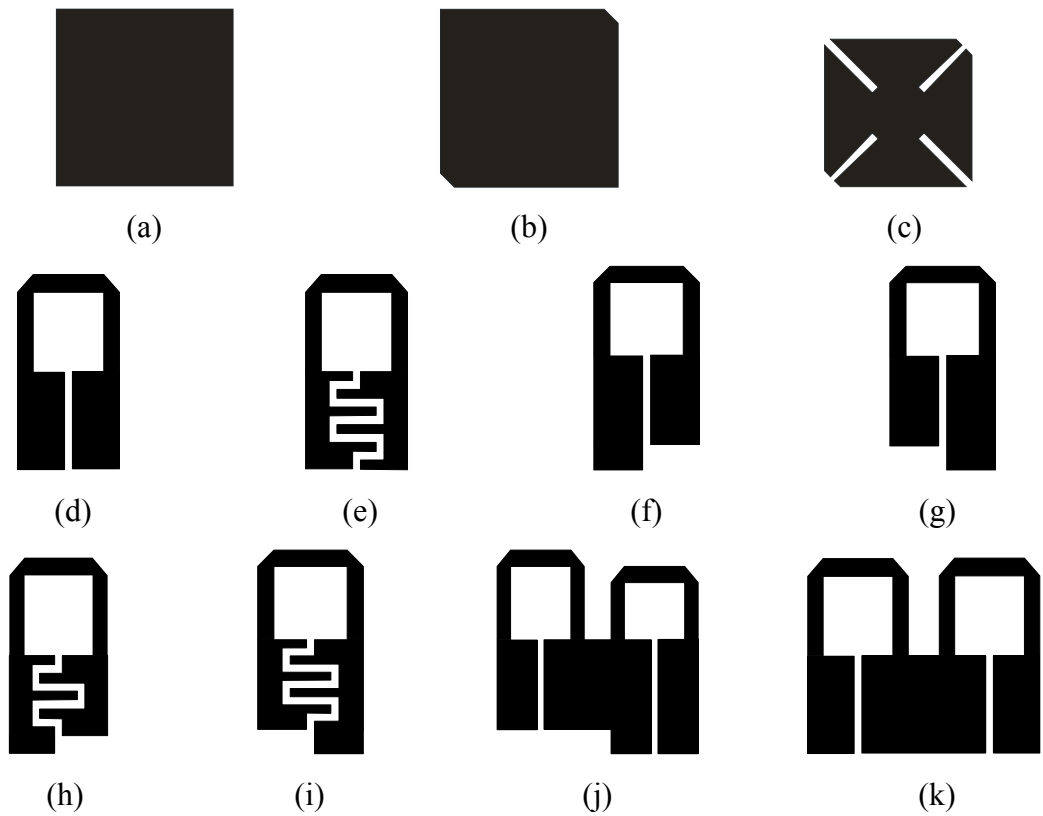
The design specifications of the antenna and the filter are listed in Tables 1.1 and 1.2, respectively. Figure 1.13 shows the geometry of the proposed antennas and filters.

Table 1.1: Design specification of the antenna.

Operating Frequency	2.45 GHz
Polarization	Circular
Voltage Standing Wave Ratio, VSWR	$1 < \text{VSWR} < 2$
VSWR Bandwidth	24 MHz
Input Return loss	< -15 dB
Axial Ratio, AR	< 3 dB
Circular Polarization Bandwidth	10 MHz

Table 1.2: Design specification of the low-pass filter.

Response	Elliptic Function
Cutoff Frequency, f_c	3 GHz
Passband ripple, L_{Ar}	-0.1 dB
Stopband Ratio, Ω_s	2
Minimum Stopband Insertion Loss, L_{As}	-24 dB
Slope	-7 dB/GHz
Insertion Loss at Second harmonic, $2f_r = 4.9$ GHz	< -20 dB
Insertion Loss at Third harmonic, $3f_r = 7.35$ GHz	< -10 dB

**Figure 1.13** Geometry of the investigated antennas and filters (not to scale).

- (a) Basic square patch, SP, (b) Corner-truncated square patch, CTSP,
(c) Slitted corner-truncated square patch, SCTSP, (d) Single stepped-impedance hairpin, SIH,
(e) Meandered-gap hairpin, MGH, (f) Left over-coupled end hairpin, OCEH_L,
(g) Right over-coupled end hairpin, OCEH_R, (h) Left over-coupled end MGH, OCEMGH_L,
(i) Right over-coupled end MGH, OCEMGH_R, (j) Unidentical cascaded hairpin, UCH,
(k) Identical cascaded hairpin, ICH.

Microstrip configuration was chosen as the planar structure for the antenna and low-pass filter. The microstrip has advantages of being light weight, low profile, flat form and can be easily integrated with other electronic circuitry [24, 31, 21]. The antenna is designed to have circular polarization which can eliminate the need to orient the antenna, reduce the effect of multipath and maximize the received signal. Corner-truncated square patch is chosen as the configuration for the antenna to achieve circular polarization with single feed. EF response is chosen for the filter to achieve sharp roll-off cutoff frequency and higher stopband rejections.

The research contributions are reflected in the design of the following front-end elements:

- (i) circularly polarized SCTSP with EMC feed,
- (ii) single SIH EF-LPF,
- (iii) single MGH EF-LPF,
- (iv) OCEMGH EF-LPF,
- (v) UCH and ICH EF-LPFs and
- (vi) single front-end rectenna prototype elements; SCTSP and a single OCEMGH EF-LPF.

1.6 Thesis Organization

This thesis is organized into 8 chapters. Chapter 1 introduces the research work which includes the background, objective, scope, contribution of the research and problem statement. Literature review of the front-end rectenna is also presented.

Chapter 2 covers the basic theory of the square patch microstrip antenna, the feeding techniques used, CTSP antenna and reviews of the compact microstrip antenna.

Chapter 3 covers the basic theory of the elliptic function LPF, coupled microstrip lines and reviews of the microstrip elliptic function LPF.

Chapter 4 discusses the design of the slitted CTSP. Initially, one layer square patch fed by coaxial feed is designed. Then slitted CTSP fed by EMC feed was designed to operate at 2.45 GHz. Two scaled down designs of 1.5 and 2 of slitted CTSP were also presented. Simulation results were presented and discussed.

Chapter 5 discusses the design of the hairpin elliptic function LPF of 3rd order. Three designs were presented and their simulated performances were analyzed.

In Chapter 6, the design of the cascaded hairpin elliptic function LPF of 5th order is discussed. Two designs were presented and their simulated performances were analyzed.

The experimental testing of the designed antenna and LPF were presented in Chapter 7. The results and analysis were also presented.

The final chapter concludes the thesis. Recommendations and suggestions for future work were also presented.

REFERENCES

1. Yoo, T. W. and Chang, K. (1992). Theoretical and experimental development of 10 and 35 GHz rectennas. *IEEE Trans. MTT*, 40(16), 1259-1266.
2. Dickinson, R. M. (2003). Wireless power transmission technology state of the art the first Bill Brown lecture. *Acta Astronautica*, 53, 561-570.
3. Brown, W. C. (1984). The history of power transmission by radio waves. *IEEE Trans. MTT*, 32(9), 1230-1242.
4. Goswami, D. Y., Vijayaraghavan, S., Lu, S. and Tamm, G. (2004). New and emerging developments in solar energy. *Elsevier, Solar Energy*, 73, 33-43.
5. Akkermans, J. A. G, vanBeurden, M. C., Doodeman, G. J. N. and Visser, H. J. (2004). Analytical models for low-power rectenna design. *IEEE Antennas Wireless Propagat. Lett.*, 4, 187-190.
6. Brown, W. C. and Triner, J. F. (1982). Experimental thin-film etched-circuit rectenna. *IEEE MTT-S Int. Microwave Symp. Dig.*, 82(1), 185-187.
7. Schlesak, J., Alden, A., and Ohno, T. (1988). A microwave powered high altitude platform. *IEEE MTT-S Microwave Symp. Dig.*, 1, 283-286.
8. Yoo, T., McSpadden, J. O. and Chang, K. (1992). 35 GHz rectenna implemented with a patch and a microstrip dipole antenna. *IEEE MTT-S Digest*, 1, 345-347.
9. McSpadden, J. O., Fan, L. and Chang, K. (1997). A high conversion efficiency 5.8 GHz rectenna. *IEEE MTT-S Digest*, 2, 547-550.
10. Na, Y.-S, Kim, J.-S., Kang, Y.-C, Byeon, S.-G. and Rha, K.-H. (2004). Design of a 2.45 GHz passive transponder using printed dipole rectenna for RFID application. *TENCON IEEE Region 10 Conference, C*, 547-549.
11. Suh, Y.H. and Chang, K. (2002). A high efficiency dual frequency rectenna for 2.45 and 5.8 GHz wireless power transmission. *IEEE Trans. MTT*, 50(7),1784-1789.

12. McSpadden, J. O. and Chang, K. (1998). A dual polarized circular patch rectifying antenna at 2.45 GHz for microwave power conversion and detection. *IEEE MTT-S Int. Microwave Symp. Dig.*, 3, 1749-1752.
13. Fujino, Y., Kaya, N., and Saka, T. (2002). Development of C-band rectenna for microwave power transmission toward a space robot. *Acta Astronautica*, 50, 295-300.
14. Youn, D. G, Park, Y. H., Kim, K. H. and Rhee, Y. C. (1999). A study on the fundamental experiment for wireless power transmission system. *Proc. Of the IEEE Region 10 Conference, TENCON 99*, 2, 1419-1422.
15. Heikkinen, J., Salonen, P., and Kivikoski, M. (2000). Planar rectennas for 2.45 GHz wireless power transfer. *IEEE RAWCON, Radio and Wireless Conference*, 63-66.
16. Park, J.-Y., Han, S.-M. and Itoh, T. (2004). A rectenna design with harmonic-rejecting circular sector antenna. *IEEE Ant. Wireless Propagat. Lett.*, 3, 52-54.
17. Han, S.-M., Park, J.-Y. and Itoh, T. (2004). Dual-fed circular sector antenna system for a rectenna and a RF receiver. *34th European Microwave Conference, IEEE*, 2, 1089-1092.
18. Rasshofer, R. H., Thieme, M. O. and Biebl, E. M. (1998). Circularly polarized millimeter-wave rectenna on silicon substrate. *IEEE Trans. MTT*, 46(5), 715-718.
19. Strassner, B. and Chang, K. (2003). Highly efficient C-band circularly polarized rectifying antenna array for wireless microwave power transmission. *IEEE Trans. Antennas Propagat.* 51(6), 1347-1355.
20. Heikkinen, J. and Kivikoski, M. (2004). Low-profile circularly polarized rectifying antenna for wireless power transmission at 5.8 GHz. *IEEE Micro. Wireless Comp. Lett.*, 14(4), 162-164.
21. Suh, Y.H., Wang, C., and Chang, K. (2000). Circularly polarized truncated-corner square patch microstrip rectenna for wireless power transmission." *Electronics Letters*, 36(7), 600-602.
22. Xu, J., Xu, D., Yang, X. Xu, C. (2004). Analysis and design of microstrip antenna for rectenna of in-pipe micromachine using FDTD method. *IEEE Antennas Propagat. Society Symp.*, 1, 1082-1085.
23. Osepchuk, J. M. (2002). How Safe Are Microwaves and Solar Power from Space? *IEEE Microwave Magazine*, 58-64.

24. Sainati, R. A. (1996). *CAD of Microstrip Antennas for Wireless Applications*. Norwood, MA: Artech House.
25. Chin, C.-H.K., Xue, Q. and Chan, C.H. (2005). Design of a 5.8 GHz rectenna incorporating a new patch antenna. *IEEE Antennas Wireless Propagat. Lett.* 4, 175-178.
26. Mathcad 2000 Professional. Mathsoft. Massachusetts. USA.
27. www.mwoffice.com, March 2004.
28. Sonnet Software Inc. (2003). *Sonnet User's Guide, Release 9*. New York.
29. AntennaLab. (1994). *Operation Manual*. FeedBack Instrument Ltd. England.
30. Microstrip Trainer. (1994). *Operation Manual*. FeedBack Instrument Ltd. England.
31. Balanis, C. A. (2005). *Antenna Theory: Analysis and Design*. 3rd edition. Canada: Wiley.
32. Hong, J. S. and Lancaster, M. J. (2001). *Microstrip Filer for RF/Microwave Application*. USA: Wiley.
33. Pozar, D. M. (2004). *Microwave Engineering*. 3rd ed. Canada: Wiley.
34. Stutzman, W. L. and Thiele, G. A. (1998). *Antenna Theory and Design*. 2nd edition. USA: Wiley.
35. White, F. J. (2004). *High Frequency Techniques: An Introduction to RF and Microwave Engineering*. Hoboken, N. J.: Wiley.
36. Stutzman, W. L. (1993). *Polarization in Electromagnetic Systems*. Norwood, MA: Artech House.
37. Wong, K.-L. (2002). *Compact and Broadband Microstrip Antenna*. New York: Wiley.
38. Kraus, J. D. and Marhefka, R. J. (2002). *Antennas for All Applications*. Third edition. New York: McGraw-Hill.
39. Evans, G. E. (1990). *Antenna Measurement Techniques*. Norwood, MA: Artech House.
40. Toh, B. Y., Cahill, R. and Fusco, V. F. (2003). Understanding and measuring circular polarization. *IEEE Trans. Educ.*, 45(3), 313-318
41. Strassner, B. and Chang, K. (2003). 5.8 GHz circularly polarized dual-rhombic-loop traveling-wave rectifying antenna for low power-density wireless power transmission applications. *IEEE Trans. MTT*, 51(5), 1548-1553.

42. Bhartia, P., Rao, K. V. S. and Tomar, R. S. (1991). *Millimeter-Wave Microstrip and Printed Circuit Antennas*. Norwood, MA: Artech House, Inc.
43. Wong, K.-L. (2003). *Planar Antennas for Wireless Communications*. New Jersey: Wiley.
44. Hirasawa, K. and Haneishi, M. (1992). *Analysis, Design, and Measurement of Small and Low-Profile Antennas*. Norwood, MA: Artech House.
45. Pozar, D. M. and Schaubert, D. H. (1995). *The Analysis and Design of Microstrip Antennas and Arrays*. A Selected Reprint Volume. IEEE Antennas and Propagation Society Sponsor. New York.
46. Bahl, I. J. and Bhartia, P. (1980). *Microstrip Antennas*. Massachusetts: Artech House.
47. Wadell, B. C. (1991). *Transmission Line Design Handbook*. Norwood, MA: Artech House.
48. James, J.R. and Hall, P.S. (1989). *Handbook of Microstrip Antennas*. London, UK: Peter Peregrinus.
49. Chen, W.-S., Wu, C.-K. and Wong, K.-L. (1998). Single-feed square-ring microstrip antenna with truncated corners for compact circular polarisation operation. *Electron. Lett.*, 34(11), 1045-1047.
50. Wong, K.-L. and Wu, J.-Y. (1997). Single-feed small circularly polarized square microstrip antenna. *Electron. Lett.*, 33(22), 1833-1834.
51. Wong, K.-L. and Lin, Y.-F. (1997). Small broadband rectangular microstrip antenna with chip-resistor loading. *Electron. Lett.*, 33(19), 1593-1594.
52. _____. (1998). Circularly polarized microstrip antenna with a tuning stub. *Electron. Lett.*, 32(9), 831-832.
53. Chen, W.-S., Wu, C.-K. and Wong, K.-L. (2001). Novel compact circularly polarized square microstrip antenna. *IEEE Trans. Antenna and Propagat.*, 49(3), 340-341.
54. William, A. B. and Taylor, F. J. (1995). *Electronic Filter Design Handbook*. Third ed. New York: McGraw-Hill.
55. Das, A. and Das, S. K. (2000). *Microwave Engineering*. New Delhi: Tata McGraw-Hill.
56. Gupta, K. C., Garg, R., Bahl, I. and Bhartia, P. (1996). *Microstrip Lines and Slotlines*. Second ed. Norwood, MA: Artech House.

57. Garg, R. and Bahl, I. J. (1979). Characteristics of coupled microstrip lines. *IEEE Trans. MTT-27*, 700-705. Corrections in (1980), *IEEE Tran. MTT-28*, p. 272.
58. Kirschning, M. and Jansen, R. H. (1984). Accurate wide-range design equations for parallel coupled lines. *IEEE Trans. MTT-32*, Jan. 1984, 83-90. Correction in *IEEE Trans. MTT-33*, March 1985, p. 288.
59. Giannini, F., Salerno, M. and Sorrentino, R. (1982). Design of low-pass elliptic filters by means of cascaded microstrip rectangular elements. *IEEE Trans. MTT.*, 30(9), 1348-1353.
60. Sheen, J.-W. (2000). A compact semi-lumped low-pass filter for harmonic and spurious suppression. *IEEE Microwave Guided Wave Lett.*, 10(3), 92-93.
61. Yang, N., Chen, Z. N., Wang, Y. Y. and Chia, M. Y. W. (2003). An elliptic low-pass filter with shorted cross-over and broadside-coupled microstrip lines. *IEEE MTT-S Digest*, 535-538.
62. Jianxin, C., Mengxia, Y., Jun, X. and Quan, X. (2004). Compact microstrip lowpass filter. *Electronic Lett.* 40(11).
63. Hsieh, L.-H. and Chang, K. (2003). Compact, broad-stopband elliptic-function lowpass filter using microstrip stepped impedance hairpin resonator. *IEEE MTT-S Dig.*, 3, 1775-1778.
64. www.rogerscorporation.com, January 2004.
65. Garg, R., Bhartia, P., Bahl. and Ittipoboon, A. (2001). *Microstrip Antenna Design Handbook*. USA: Artech House.
66. Splitt, G. and Davidovitz, M. (1990). Guidelines for Design of Electromagnetically Coupled Microstrip Patch Antennas on Two-Layer Substrates. *IEEE Trans. MTT*, 38(7), 1136-40.
67. Belentepe, B. (1995). Modeling and design of electromagnetically coupled microstrip-patch antennas and antenna arrays. *IEEE Antennas Propagat. Magazine*, 37(1), 31-39.
68. Wu, D. and Huang, J. (1994). CAD and optimization of circularly-polarized microstrip arrays. *IEEE Antennas Propagat. Society Int'l Symp.*, 3, 1840-43.
69. Langston, W. L. and Jackson, D. R. (2004). Impedance, axial-ratio, and receive-power bandwidths of microstrip antennas. *IEEE Trans. Antennas Propagat.*, 52(10), 2769-2773.

70. Ali, M. I., Ehata, K. and Ohshima, S. (1999). Superconducting patch array on both-side YBCO thin film for satellite communication. *IEEE Trans. Applied Superconduct.*, 9(2), 3077-3080.
71. Hamid, M. R. (2001). Printed Antenna for Bluetooth Application. Master Thesis. Universiti Teknologi Malaysia.
72. Laheurte, J. M. (2003). Dual-frequency circularly polarized antennas based on stacked monofilar square spirals. *IEEE Trans. Antennas Propagat.*, 51(3), 488-492.
73. Sagawa, M., Takahashi, K. and Makimoto, M. (1989). Miniaturized hairpin resonator filter and their application to receiver front-end MIC's. *IEEE Trans. MTT*, 37(2), 1991-1997.
74. Kim, B. S. Lee, J. W. and Song, M. S. (2003). Modified microstrip filters improving the suppression performance of harmonic signals. *IEEE MTT-S Dig.*, 539-542.
75. Hsieh, L.-H. and Chang, K. (2001). Compact lowpass filter using stepped impedance hairpin resonator. *Electron. Lett.*, 37(14), 899-900.
76. Riddle, A. (1988). High performance parallel coupled microstrip filters. *IEEE MTT-S Symp Dig.*, 427-430.
77. Kuo, J. T., Chen, S. P. and Jiang M. (2003). Parallel-coupled microstrip filters with over-coupled end stages for suppression of spurious responses. *IEEE Microwave Wireless Comp. Lett.*, 13(10), 440-442.
78. Bahl, I. J. (1989). Capacitively compensated high performance parallel coupled microstrip filters, *IEEE MTT-S Symp Dig.*, 679-682.
79. Kuo, J. T., Hsu, W. H. and Huang, W. T. (2002). Parallel coupled microstrip filters with suppression of harmonic response. *IEEE Microwave Wireless Comp. Lett.*, 12, 383-385.
80. Kim, B. S. Lee, J. W. and Song, M. S. (2004) An implementation of harmonic-suppression microstrip filters with periodic grooves. *IEEE Microwave Wireless Comp. Lett.*, 1-3.
81. Mazzarella, G. (1999). CAD modeling of interdigitated structures. *IEEE Trans. Educ.*, 42(1), 81-87.
82. Strassner, B. and Chang, K. (2000). 5.8 circular polarized rectenna for microwave power transmission, *IECEC Energy Conversion Engg. Confer. Exhibit*, 2, 1458-1468.